

# Self-Assembling All-Enzyme Hydrogels for Flow Biocatalysis

Theo Peschke, Patrick Bitterwolf, Sabrina Gallus, Yong Hu, Claude Oelschlaeger, Norbert Willenbacher, Kersten S. Rabe, and Christof M. Niemeyer\*

**Abstract:** Continuous flow biocatalysis is an emerging field of industrial biotechnology that uses enzymes immobilized in flow channels for the production of value-added chemicals. We describe the construction of self-assembling all-enzyme hydrogels that are comprised of two tetrameric enzymes. The stereoselective dehydrogenase LbADH and the cofactor-regenerating glucose 1-dehydrogenase GDH were genetically fused with a SpyTag or SpyCatcher domain, respectively, to generate two complementary homo-tetrameric building blocks that polymerize under physiological conditions into porous hydrogels. Mounted in microfluidic reactors, the gels show excellent stereoselectivity with near quantitative conversion in the reduction of prochiral ketones along with high robustness under process and storage conditions. The gels function as compartment that retains intermediates thus enabling high total turnover numbers of the expensive cofactor NADP(H).

**B**iocatalysis is a green and sustainable technology that is widely considered as a key domain of industrial (“white”) biotechnology, which is expected to have an enormous impact on the emergence of biobased economy.<sup>[1]</sup> Towards this goal, bioinspired, multistep enzymatic cascade reactions are currently attracting much attention.<sup>[2]</sup> Their exploitation for technical processes requires compartmentalized flow systems to prevent multiple reactions from spreading and unproductive crosstalk. While this approach is well implemented in “continuous flow chemistry” that has yielded impressive synthesis campaigns for small molecules,<sup>[3]</sup> the implementation of enzyme-based production processes, i.e., continuous flow biocatalysis, is far less developed.<sup>[2g,4]</sup>

Biocatalytic flow processes are difficult to realize because the heterogeneous catalysis regime calls for effective surface immobilization techniques that are more demanding for enzymes than for conventional organo(metallic) catalysts.<sup>[5]</sup> Common methods for enzyme immobilization inside microstructured flow channels, such as physisorption, chemical cross-linking, or genetically encoded immobilization tags,<sup>[6]</sup>

have proven their applicability,<sup>[2g,4c-g]</sup> however, there remains the problem that the amount of immobilized biocatalyst is limited by the effective surface area. To overcome this limitation, pseudo-3D interfacial layers comprised of synthetic polymers or micro-/nanoparticles<sup>[7]</sup> can be used to increase the loading capacity for enzymes.<sup>[8]</sup> These approaches also waste the limited reactor space and also often require additional coupling steps with potential drawbacks for biocatalytic activity. Therefore, in situ generation of pure enzyme hydrogels would provide an ideal solution for the loading with maximum possible quantities of active biocatalyst. Hydrogels are porous polymers that can be constructed from natural or synthetic structural proteins.<sup>[9]</sup> A recently established protein gelation strategy utilizes a pair of genetically encoded reactive partners, SpyTag and SpyCatcher, that spontaneously form a covalent isopeptide linkage under physiological conditions.<sup>[10]</sup> While these protein hydrogels are being explored for applications in biomedical sciences, such as cell encapsulation and tissue engineering, strategies for their exploitation in biocatalysis remain underdeveloped.

We here present a self-assembling all-enzyme hydrogel that displays high space-time yields in biocatalytic flow processes. We choose two widely used homotetrameric enzymes, the highly (R)-selective alcohol dehydrogenase (EC 1.1.1.2) from *Lactobacillus brevis* (LbADH) and the nicotinamide adenine dinucleotide phosphate (NADPH)-regenerating glucose 1-dehydrogenase GDH (EC 1.1.1.47) from *Bacillus subtilis*. Both enzymes were genetically fused with either the SpyTag (ST) or the SpyCatcher (SC) in addition to a hexahistidin (His) tag tethered to the same terminus of the protein (Figure 1a). Given the molecular weights of LbADH, GDH, His-SC and ST-His (27, 28, 13 and 3 kDa, respectively), this leads to a hydrogel whose mass consists of 77% enzymes. The ST/SC system enables the rapid cross-linking of the two tetravalent protein building blocks through the formation of covalent isopeptide bonds under physiological conditions.<sup>[11]</sup> The proteins were overexpressed in *E. coli* and purified to homogeneity by Ni-NTA affinity chromatography (Figure S1 in the Supporting Information). Initial electrophoretic analysis of enzyme gelation confirmed that polymerization only occurs when both enzymes bear the complementary binding sites (Figure S2). A more detailed investigation of the polymerization reaction by dynamic light scattering (DLS) analysis (Figure 1b,c) revealed that the time-dependent formation of protein clusters occurred on time scales of minutes to hours, depending on the concentration of the two enzyme building blocks (Figure 1b). In homogeneous solution particles with average size of up to 65 nm were formed that further fused to a viscous liquid and even free-standing hydrogel pieces upon further desiccation

[\*] Dr. T. Peschke, M. Sc. P. Bitterwolf, M. Sc. S. Gallus, M. Sc. Y. Hu, Dr. K. S. Rabe, Prof. Dr. C. M. Niemeyer  
Karlsruhe Institute of Technology (KIT)  
Institute for Biological Interfaces (IBG 1)  
Hermann-von-Helmholtz-Platz 1  
76344 Eggenstein-Leopoldshafen (Germany)  
E-mail: niemeyer@kit.edu  
Dr. C. Oelschlaeger, Prof. Dr. N. Willenbacher  
Karlsruhe Institute of Technology (KIT)  
Institute for Mechanical Process Engineering and Mechanics  
Gotthard-Franz-Strasse 3, 76131 Karlsruhe (Germany)

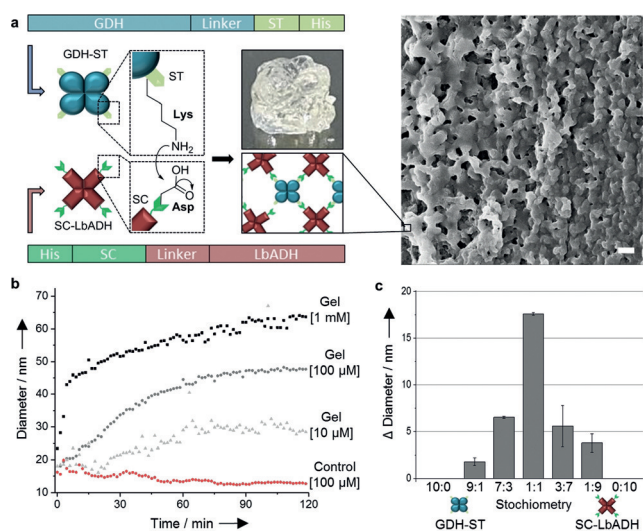


**Figure 1.** Design, formation and morphological characterization of the self assembled all enzyme hydrogels. a) Schematic illustration of the two homotetrameric enzyme building blocks, GDH ST and SC LbADH, that can self assemble to a hydrogel via formation of covalent isopeptide bonds. Photograph and representative SEM image of the hydrogel; scalebar 300 nm; for additional morphological characterization see Figure S3. b) Time and concentration dependent increase in hydrodynamic diameter (Z average), determined at 25 °C by DLS. The control contained equimolar amounts of GDH ST and LbADH lacking the SC domain. c) Stoichiometry dependent increase in particle diameter observed in the initial 30 min after mixing of the two enzyme building blocks (100 μM total subunit concentration, 25 °C).

of the solvent (Figure 1 a,b). Variation of the stoichiometric ratio of the two enzyme building blocks showed the fastest increase of the hydrodynamic diameter at equimolar ratio (Figure 1c). Analysis of the gel's morphology by scanning electron microscopy (SEM) and atomic force microscopy (AFM) revealed no clearly distinctive ultrastructure, however, particle like features were evident in both SEM and AFM images (Figure 1 a, S3).

To further elucidate the material properties, the enzyme hydrogels were analyzed by optical micro rheology based on multiple particle tracking (MPT) analysis<sup>[12]</sup> (Figure S4). The method revealed that the hydrogel has a homogeneous structure on the micrometer length scale with a  $G_0 = 20 \pm 7$  Pa, an average mesh size  $\xi = 60 \pm 7$  nm and a pore size  $< 200$  nm. Since the pore size is in the range of typical microfiltration membranes,<sup>[13]</sup> the gels should be well suited for flow reactions.

Owing to its relevance for stereochemistry and natural product synthesis,<sup>[14]</sup> we chose the prochiral  $C_s$  symmetrical 5 nitrononane 2,8 dione (NDK) **1** (Figure 2a) as the substrate for benchmarking the biocatalytic activity of the all enzyme hydrogels. Depending on the stereoselectivity of a given ketoreductase, either one or both carbonyl groups of NDK are reduced to form diastereomeric hydroxyketones **2** or diols **3**, respectively (see also Figure S5), and all products can be readily quantified by chiral HPLC analysis.<sup>[14a]</sup> We had previously established that particle immobilized LbADH converts NDK with very high stereoselectivity into (*R*) *syn/anti* hydroxyketones **2c/d** (e.r.  $> 99:1$ ; d.r.  $\approx 60:40$ ), which are

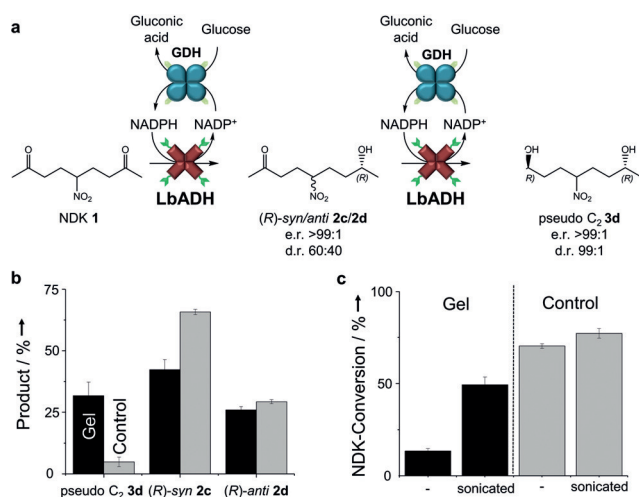


**Figure 2.** NDK reduction employing the GDH ST/SC LbADH hydrogel or unassembled enzymes (control). a) Reaction Scheme of the (*R*) selective conversion of NDK **1** to (*R*) *syn/anti* **2c/d** hydroxyketone which is further reduced to (*R,R*) configured pseudo  $C_2$  diol **3d**. b) Distribution of all reaction products after 2 hours. Note that the hydrogel rapidly reduces NDK **1** to diol **3d**, whereas the unassembled control enzymes predominantly form the hydroxyketones **2c/d**. A corresponding time dependent kinetic analysis is shown in Figure S8. c) NDK conversion of an assembled GDH ST/SC LbADH hydrogel (black) or the unassembled enzyme control (grey), respectively. Error bars indicate the standard deviation, obtained in at least two independent experiments.

further reduced to form the (*R,R*) configured pseudo  $C_2$  diol **3d**.<sup>[4d]</sup> We now used the NDK reaction to initially profile the SC LbADH and GDH ST building blocks, which revealed a slightly decreased (30%) and increased (22%) specific activity, respectively, as compared to the untagged enzymes (Figure S6, Table S1).

The kinetics of NDK reduction was then compared between the GDH ST/SC LbADH hydrogel and a control of the unassembled mixed proteins. To this end, hydrogels were prepared into which  $NADP^+$  was included during polymerization and solvent evaporation. After swelling of the hydrogel, reaction buffer, containing NDK and glucose, was added and product formation was monitored by chiral HPLC analysis. We found that the hydrogel was rapidly forming the (*R,R*) diol **3d**, whereas the unassembled enzymes produced almost exclusively the hydroxyketones **2c/d** (Figures 2b, S7). Moreover, the total activity of the unassembled enzyme system was higher than that of the hydrogel (Figure S7). We attribute both observations to mass transport limitations due to restricted diffusion in between the hydrogel and the surrounding medium. To confirm this hypothesis, the hydrogel matrix was broken up by sonication and, indeed, NDK conversion was almost equal to unassembled enzymes (Figure 2c).

To overcome the limited mass transport and to take advantage of the high enzyme concentrations, we evaluated the use of the gels in biocatalytic flow processes. Initial assessments showed that the gels and the unassembled enzymes have a similar stability against elevated temperature (Figure S8) and pH shifts (Figure S9). However, the gels

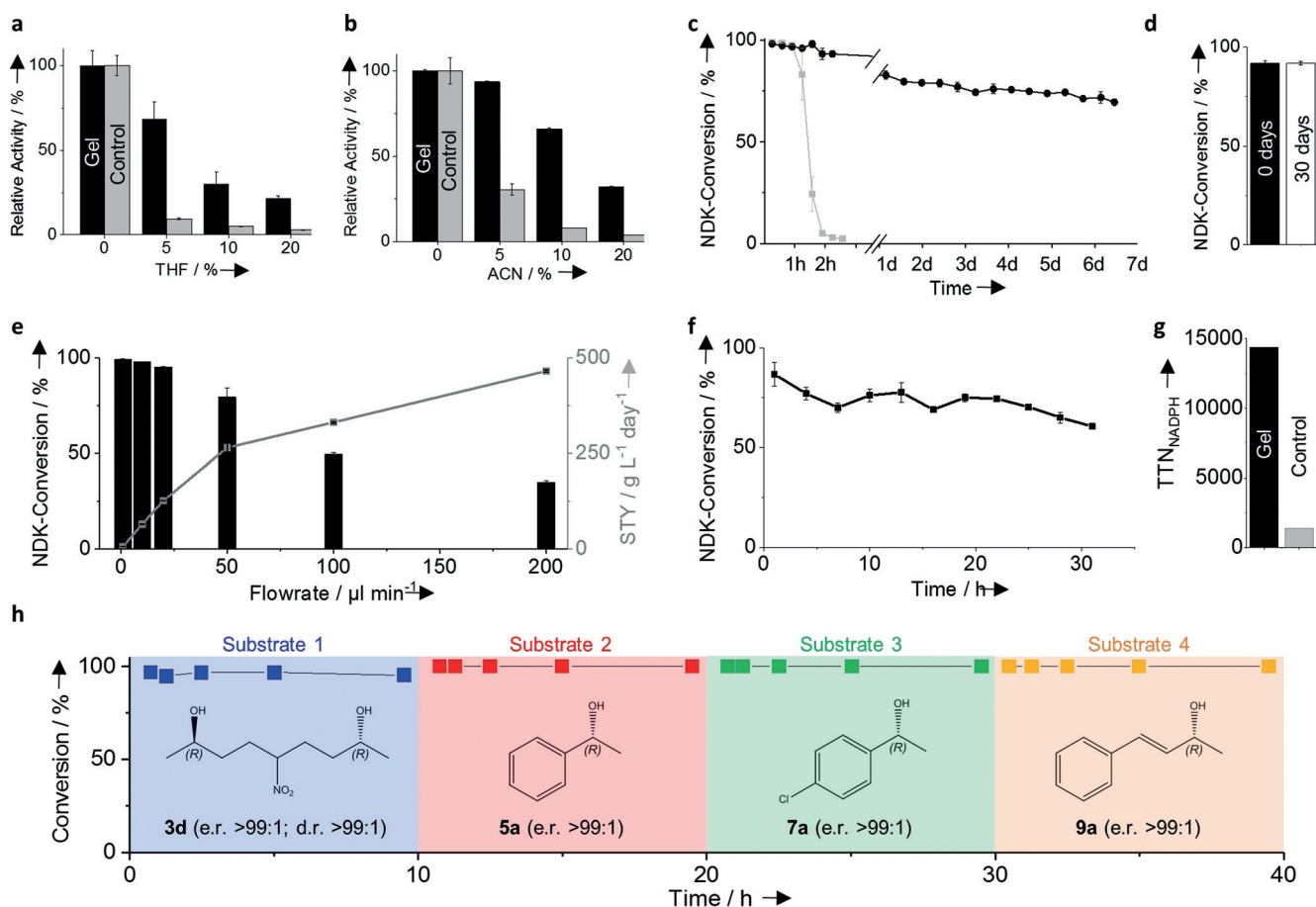


**Figure 3.** Stereoselective continuous flow biocatalysis with GDH ST/SC LbADH hydrogel loaded microfluidic reactors. a,b) Relative Activity of the hydrogel and unassembled enzymes (control) in the presence of variable concentrations tetrahydrofuran (THF), (a) and acetonitrile (ACN), (b). c) Time dependent NDK conversion, determined from the outflow of the enzyme loaded reactors perfused with continuous 5 mM substrate and continuous cofactor supply (1 mM NADP<sup>+</sup>) at a flowrate of 10  $\mu\text{L min}^{-1}$ . d) Storage stability of gel loaded reactor chips after storage for one month at 30°C. The bars show NDK conversion obtained with a fresh and stored reactor after continuous operation for one day. e) Flow rate dependent productivity (black bars) and corresponding space time yields (STY, grey line), obtained with continuous cofactor supply. f) Time dependent NDK conversion of a reactor loaded with a gel containing 1 mM entrapped NADP<sup>+</sup>, in the absence of continuous cofactor supply. g) Total Turnover Numbers of NADPH (TTN<sub>NADPH</sub>) obtained with reactors bearing polymerized hydrogels (black) or unassembled enzymes (grey). For detailed time dependent data, see Figure S11. h) Continuous flow conversion of NDK **1**, acetophenone **4**, 4'-chloroacetophenone **6** and *trans* **4** phenyl 3 buten 2 one **8** to their corresponding (*R*) configured alcohols **3d**, **5a**, **7a** and **9a** with a hydrogel loaded micro reactor. Note that conversion of **8** required addition of 1% (v/v) ACN due to its low solubility in aqueous buffers. All error bars indicate the standard deviation, obtained from at least two independent analyses.

reveal a higher tolerance against commonly used organic solvents, such as tetrahydrofuran (THF) and acetonitrile (ACN) (Figure 3a,b). We then set up a microfluidic reactor system, wherein a PDMS chip with a flow channel of 150  $\mu\text{L}$  volume was connected to syringe pumps for substrate delivery and a fraction collector for automated sampling of the outflow. The flow channel was filled with swollen hydrogel and covered with a glass slide (Figure S10).

To investigate the process stability of the GDH ST/SC LbADH hydrogels under continuous flow conditions, the channel was perfused with reaction buffer containing NADP<sup>+</sup>, glucose and NDK at a flowrate of 10  $\mu\text{L min}^{-1}$ . As expected, the hydrogel effectively retained the immobilized enzymes and showed a stable conversion of the NDK substrate for more than 6 days, whereas unassembled enzyme mixtures were rapidly washed out of the reactor (Figure 3c). Notably, hydrogel loaded chips stored for

30 days at 30°C showed a similar activity in flow experiments than freshly prepared chips (Figure 3d). This suggests that ready to use chips can be stored for prolonged times and shipped at typical conditions of 4°C. NDK conversion and corresponding space time yields (STY, Figure 3e) revealed that the reactor could be operated at 200 fold higher flowrates (200  $\mu\text{L min}^{-1}$ ; corresponding with a reactor residence time of 45 s) and performed with a > 68 fold higher time yield and a more than 4.5 fold higher STY than previously reported packed bed micro reactors that contained bead immobilized GDH and LbADH.<sup>[4d]</sup>

The fact that the hydrogel rapidly forms the (*R,R*) diol **3d** while the unassembled enzymes produced almost exclusively the hydroxyketones **2c/d** (Figure 2b, S8) suggested that intermediate species cannot easily escape from the gels due to the spatially and kinetically coupled GDH ST and SC LbADH enzymes. We reasoned that this phenomenon could

also be harnessed to prevent escape of the redox cofactor species NADP(H) from the gel under flow conditions. To investigate this hypothesis, microreactors were loaded with hydrogels bearing 1 mM co-entrapped NADP<sup>+</sup> and perfused with reaction buffer containing only glucose and NDK. Indeed, the NDK was continuously converted for more than 30 h, indicating the effective retainment of the entrapped cofactor inside the hydrogel over  $\geq 124$  reactor column volumes (Figure 3 f). By decreasing the NADP concentration to 1  $\mu$ M the total turnover number of NADPH (TTN<sub>NADPH</sub>) was greater than 14000 (Figure 3 g, S11). This is more than 13 fold higher than that of a recently reported self-sufficient heterogeneous biocatalyst, based on bead-bound ketoreductases with electrostatically co-immobilized NADP(H).<sup>[15]</sup> To the best of our knowledge, the TTN<sub>NADPH</sub> observed here is the highest value ever reported for flow processes in devices lacking supportive membranes, thereby clearly meeting the demands determined for economically feasible processes.<sup>[16]</sup>

As a further demonstration of the hydrogels' utility for applications in continuous flow biocatalysis, hydrogel-loaded microreactors were used for continuous production of chiral (*R*)-configured alcohols (Figure 3 h). To this end, the chip was sequentially perfused with solutions of four different methyl ketone substrates that were converted to their respective (*R*)-alcohols (**3d**, **5a**, **7a** and **9a**, in Figure 3 h). Each substrate administration was conducted for 10 h and reaction products in the outflow were analyzed by chiral HPLC. We found that all substrates were reduced to the corresponding (*R*)-configured alcohols with near-quantitative conversion and stereoselectivities of >99%. These results clearly show that the novel biocatalytic hydrogels hold a large potential for real-life laboratory applications.

In conclusion, we established a novel class of self-assembled all-enzyme hydrogels that are convenient to prepare and readily mounted in fluidic microreactors. Conventional (multi)enzyme processes require carrier materials, such as beads or membranes, which inevitably "dilute" the specific activity of a given device and, thus, lead to lower STYs than those available with all-enzyme systems.<sup>[1b,17]</sup> Our approach is based on recombinant protein technology, thereby enabling the "green" sustainable production of biocatalytic devices with high catalyst and volume productivity, high stability and low production costs owing to the exclusion of additional expensive carrier materials that require additional efforts for production and disposal. The ultimately high concentrations of the biocatalyst in our hydrogels are comparable only to the so-called "cross-linked enzyme aggregates" (CLEA) that can be produced from two or more different proteins in a non-directional fashion by glutaraldehyde-mediated unselective cross-linking<sup>[18]</sup> or by exploitation of metal coordination interactions.<sup>[19]</sup> These approaches, however, are limited in terms of control over enzyme stoichiometry, potentially adverse effects of the chemical crosslinking on the enzyme activity, or sensitivity to environmental conditions (e.g., pH and ion strength of reaction media).

Since the industrial implementation of enzymatic flow processes is difficult when expensive cofactors (e.g., NADPH) need to be supplemented continuously,<sup>[20]</sup> our

approach should also be relevant for other important biocatalysts, such as P450 monooxygenases,<sup>[21]</sup> imine reductases<sup>[22]</sup> or transaminases.<sup>[23]</sup> Conventional approaches for cofactor retainment in flow systems use ultra- and nano-filtration membranes or specifically modified surfaces that retain cofactors through electrostatic attraction or even covalent immobilization. While these approaches have led to increased TTN<sub>NADPH</sub> values, they can increase the complexity of production processes and costs, thereby leading to limited economic viability.<sup>[15,24]</sup> Our self-assembly approach, in contrast, is straightforward, scalable<sup>[25]</sup> and, owing to the gel's intrinsic material properties, can be readily implemented in arbitrary reactor geometries. We therefore believe that this work paves the way for the development of novel catalytic biomaterials for applications in continuous flow biocatalysis.

## Acknowledgements

This work was supported by the Helmholtz programme "BioInterfaces in Technology and Medicine" and DFG project Ni399/15-1. PB and SG are grateful for a Kekulé fellowship by Fonds der Chemischen Industrie. We thank Ishtiaq Ahmed, Jens Bauer, Anke Dech, Leonie Hacker, Silla Hansen, Arnold Leidner, Esther Mittmann, Hatice Mutlu and Volker Zibat (LEM) for experimental help.

## Conflict of interest

The authors declare no conflict of interest.

**Keywords:** enzymes · flow biocatalysis · immobilization · microreactors · stereoselective reactions

- [1] a) A. J. Straathof, *Chem. Rev.* **2014**, *114*, 1871–1908; b) R. A. Sheldon, J. M. Woodley, *Chem. Rev.* **2018**, *117*, 801–838.
- [2] a) A. H. Chen, P. A. Silver, *Trends Cell. Biol.* **2012**, *22*, 662–670; b) I. Wheeldon, S. D. Minter, S. Banta, S. C. Barton, P. Atanassov, M. Sigman, *Nat. Chem.* **2016**, *8*, 299–309; c) A. Kuchler, M. Yoshimoto, S. Luginbuhl, F. Mavelli, P. Walde, *Nat. Nanotechnol.* **2016**, *11*, 409–420; d) Z. Chen, A. P. Zeng, *Curr. Opin. Biotechnol.* **2016**, *42*, 198–205; e) M. B. Quin, K. K. Wallin, G. Zhang, C. Schmidt Dannert, *Org. Biomol. Chem.* **2017**, *15*, 4260–4271; f) S. P. France, L. J. Hepworth, N. J. Turner, S. L. Flitsch, *ACS Catal.* **2017**, *7*, 710–724; g) K. S. Rabe, J. Muller, M. Skoupi, C. M. Niemeyer, *Angew. Chem. Int. Ed.* **2017**, *56*, 13574–13589; *Angew. Chem.* **2017**, *129*, 13760–13777.
- [3] a) S. V. Ley, D. E. Fitzpatrick, R. J. Ingham, R. M. Myers, *Angew. Chem. Int. Ed.* **2015**, *54*, 3449–3464; *Angew. Chem.* **2015**, *127*, 3514–3530; b) J. Li, S. G. Ballmer, E. P. Gillis, S. Fujii, M. J. Schmidt, A. M. Palazzolo, J. W. Lehmann, G. F. Morehouse, M. D. Burke, *Science* **2015**, *347*, 1221–1226; c) A. Adamo, R. L. Beingsner, M. Behnam, J. Chen, T. F. Jamison, K. F. Jensen, J. C. Monbaliu, A. S. Myerson, E. M. Revalor, D. R. Snead, T. Stelzer, N. Weeranoppanant, S. Y. Wong, P. Zhang, *Science* **2016**, *352*, 61–67; d) M. B. Plutschack, B. Pieber, K. Gilmore, P. H. Seeberger, *Chem. Rev.* **2017**, *117*, 11796–11893.

- [4] a) S. Matosevic, N. Szita, F. Baganz, *J. Chem. Technol. Biotechnol.* **2011**, *86*, 325–334; b) R. Wohlgemuth, I. Plazl, P. Znidarsic Plazl, K. V. Germaey, J. M. Woodley, *Trends Biotechnol.* **2015**, *33*, 302–314; c) L. Tamborini, P. Fernandes, F. Paradisi, F. Molinari, *Trends Biotechnol.* **2018**, *36*, 73–88; d) T. Peschke, M. Skoupi, T. Burgahn, S. Gallus, I. Ahmed, K. S. Rabe, C. M. Niemeyer, *ACS Catal.* **2017**, *7*, 7866–7872; e) J. Britton, R. P. Dyer, S. Majumdar, C. L. Raston, G. A. Weiss, *Angew. Chem. Int. Ed.* **2017**, *56*, 2296–2301; *Angew. Chem.* **2017**, *129*, 2336–2341; f) J. Britton, S. Majumdar, G. A. Weiss, *Chem. Soc. Rev.* **2018**, *47*, 5891–5918; g) M. L. Contente, F. Paradisi, *Nat. Catal.* **2018**, *1*, 452–459.
- [5] K. Buchholz, V. Kasche, U. T. Bornscheuer, *Biocatalysts and Enzyme Technology*, 2nd ed., Wiley Blackwell, Weinheim, **2012**.
- [6] P. Jonkheijm, D. Weinrich, H. Schroeder, C. M. Niemeyer, H. Waldmann, *Angew. Chem. Int. Ed.* **2008**, *47*, 9618–9647; *Angew. Chem.* **2008**, *120*, 9762–9792.
- [7] a) K. Szymańska, W. Pudło, J. Mrowiec Białoń, A. Czardybon, J. Kocurek, A. B. Jarzębski, *Microporous Mesoporous Mater.* **2013**, *170*, 75–82; b) P. R. Spycher, C. A. Amann, J. E. Wehrmüller, D. R. Hurwitz, O. Kreis, D. Messmer, A. Ritler, A. Küchler, A. Blanc, M. Béhé, P. Walde, R. Schibli, *ChemBioChem* **2017**, *18*, 1923–1927.
- [8] a) N. R. Mohamad, N. H. Marzuki, N. A. Buang, F. Huyop, R. A. Wahab, *Biotechnol. Biotechnol. Equip.* **2015**, *29*, 205–220; b) M. Misson, H. Zhang, B. Jin, *J. R. Soc. Interface* **2015**, *12*, 20140891; To some extent, the limitation of effective surface area can be compensated by using thin film flow reactors [4e].
- [9] a) A. M. Jonker, D. W. P. M. Lowik, J. C. M. van Hest, *Chem. Mater.* **2012**, *24*, 759–773; b) L. D. Muiznieks, F. W. Keeley, *ACS Biomater. Sci. Eng.* **2017**, *3*, 661–679.
- [10] a) F. Sun, W. B. Zhang, A. Mahdavi, F. H. Arnold, D. A. Tirrell, *Proc. Natl. Acad. Sci. USA* **2014**, *111*, 11269–11274; b) S. C. Reddington, M. Howarth, *Curr. Opin. Chem. Biol.* **2015**, *29*, 94–99; c) X. Gao, J. Fang, B. Xue, L. Fu, H. Li, *Biomacromolecules* **2016**, *17*, 2812–2819; d) X. Gao, S. Lyu, H. Li, *Biomacromolecules* **2017**, *18*, 3726–3732; e) L. Jia, K. Minamihata, H. Ichinose, K. Tsumoto, N. Kamiya, *Biotechnol. J.* **2017**, *0*, 0.
- [11] B. Zakeri, J. O. Fierer, E. Celik, E. C. Chittock, U. Schwarz Linek, V. T. Moy, M. Howarth, *Proc. Natl. Acad. Sci. USA* **2012**, *109*, E690–697.
- [12] A. Kowalczyk, C. Oelschlaeger, N. Willenbacher, *Polymer* **2015**, *58*, 170–179.
- [13] a) Y. Pouliot, *Int. Dairy J.* **2008**, *18*, 735–740; b) M. Cheryan, *Ultrafiltration and Microfiltration Handbook*, 2nd ed., Wiley, New York, **1998**.
- [14] a) M. Skoupi, C. Vaxelaire, C. Strohmann, M. Christmann, C. M. Niemeyer, *Chem. Eur. J.* **2015**, *21*, 8701–8705; b) T. C. Nugent, F. T. Najafian, H. A. Hussein, I. Hussain, *Chem. Eur. J.* **2016**, *22*, 14342–14348.
- [15] a) A. I. Benítez Mateos, E. San Sebastian, N. Rios Lombardia, F. Moris, J. Gonzalez Sabin, F. Lopez Gallego, *Chem. Eur. J.* **2017**, *23*, 16843–16852; b) S. Velasco Lozano, A. I. Benitez Mateos, F. Lopez Gallego, *Angew. Chem. Int. Ed.* **2017**, *56*, 771–775; *Angew. Chem.* **2017**, *129*, 789–793.
- [16] H. K. Chenault, E. S. Simon, G. M. Whitesides, *Biotechnol. Genet. Eng. Rev.* **1988**, *6*, 221–270.
- [17] J. M. Bolivar, D. Valikhani, B. Nidetzky, *Biotechnol. J.* **2018**, <https://doi.org/10.1002/biot.201800244>.
- [18] a) R. A. Sheldon, *Org. Process Res. Dev.* **2011**, *15*, 213–223; b) R. A. Sheldon, S. van Pelt, *Chem. Soc. Rev.* **2013**, *42*, 6223–6235.
- [19] J. D. Brodin, X. I. Ambroggio, C. Tang, K. N. Parent, T. S. Baker, F. A. Tezcan, *Nat. Chem.* **2012**, *4*, 375–382.
- [20] W. Liu, P. Wang, *Biotechnol. Adv.* **2007**, *25*, 369–384.
- [21] V. B. Urlacher, M. Girhard, *Trends Biotechnol.* **2012**, *30*, 26–36.
- [22] J. Mangas Sanchez, S. P. France, S. L. Montgomery, G. A. Aleku, H. Man, M. Sharma, J. I. Ramsden, G. Grogan, N. J. Turner, *Curr. Opin. Chem. Biol.* **2017**, *37*, 19–25.
- [23] F. Guo, P. Berglund, *Green Chem.* **2017**, *19*, 333–360.
- [24] a) K. Seelbach, U. Kragl, *Enzyme Microb. Technol.* **1997**, *20*, 389–392; b) M. Ikemi, N. Koizumi, Y. Ishimatsu, *Biotechnol. Bioeng.* **1990**, *36*, 149–154.
- [25] Scale up in microreactor technology can be conveniently achieved by “numbering up” the flow chips (B. P. Mason, K. E. Price, J. L. Steinbacher, A. R. Bogdan, D. T. McQuade, *Chem. Rev.* **2007**, *107*, 2300–2318). Based on the here reported not yet optimized dimensions and flow rates of our hydrogel microreactors, a conservative model calculation shows that for the production of 10 gram quantities of a chiral alcohol about 100 chips would have to be operated for six days.